Jiang, N., Xu, Y., Xu, T., Xu, G., Sun, C., Schuh, H. (2017): GPS/BDS short-term ISB modelling and prediction. - *GPS Solutions*, *21*, 1, pp. 163—175.

DOI: http://doi.org/10.1007/s10291-015-0513-x

GPS/BDS short-term ISB modelling and prediction

Nan Jiang[1,2,3], Yan Xu[1,2,3], Tianhe Xu[4,5], Guochang Xu[3], Zhangzhen Sun[3], Harald Schuh[1,2]

Abstract

The Chinese BeiDou Navigation Satellite System (BDS) has completed its first milestone by providing coverage of the Asia-Pacific area navigation service since December 27, 2012. With the combination of BDS, the GNSS precise point positioning (PPP) can improve its positioning accuracy, availability, and reliability. However, in order to achieve the best positioning solutions, the inter-system bias (ISB) between GPS and BDS must be resolved as precisely as possible. In this study, a one week period (GPS week 1810) of GPS/BDS observations for 18 distributed stations from the International GNSS Service (IGS) Multi-GNSS Experiment (MGEX) are processed. Primarily, the ISB is estimated by an extended Kalman filter (EKF) as a piece-wise parameter every 30 minutes. Then we generate a smoothed ISB series (ISB_s) with a sliding window median filter to reject the outliers from the original estimated ISB series (ISB_o). After analyzing the characteristics of the ISB_s, a short-term station-dependent ISB model based on a one week period is proposed in this study. This model consists of a quadratic polynomial in time and two or three periodic functions with diurnal and semi-diurnal periods. Frequency spectrum analysis is used to determine the periods of the periodic functions and the coefficients of the quadratic function and the periodic functions are estimated by least squares (LS). For model verification we compare the ISB derived from the model (ISB_m) with ISB_s (assumed the true values). The comparisons indicate an almost normal distribution. It is found that the proposed model is consistent with the true values: the root mean square (RMS) values being about 0.7 ns, and some stations are even better. This means that the short team ISB model proposed has a high fitting accuracy. Hence, it can be used for ISB prediction. Comparing the prediction ISB series (ISB_p) with ISB_s in the following week (GPS week 1811), we can draw the conclusion that the accuracy of the prediction declines with increase of the time period. The one day period precision can achieve 0.57-1.21 ns, while the accuracy of the two day prediction decreases to 0.77-1.72 ns. Hence we recommend a predicting duration of one day. The proposed model will be beneficial for subsequent GPS/BDS PPP or

Tianhe Xu (✉)

thxugie@163.com

[1] Technical University of Berlin, Strasse des 17. Juni 135, 10623 Berlin, Germany

[2] German Research Centre for Geosciences GFZ, Telegrafenberg, 14473 Potsdam, Germany

[3] Shandong University, Institute of Space Sciences, 264209 Weihai, China

[4] State Key Laboratory of Geo-information Engineering , 710054 Xi'an, China

[5] Xi'an Research Institute of Surveying and Mapping, 710054 Xi'an, China

precise orbit determination (POD) since the ISB derived from this model can be considered as a priori constraint in the PPP/POD solutions. With this a priori constraint, the convergence time can be shortened by 19.6%, 16.1%, and 2.4% in N, E, and U components, respectively. The accuracy of result in the E component is remarkably improved by 11.9%.

Keywords Inter-system bias (ISB) BeiDou GPS Frequency spectrum analysis MGEX Precise point positioning

Introduction

Research on Precise Point Positioning (PPP) using multi-GNSS observations has become increasingly popular. It is expected that multi-GNSS PPP will improve its solution accuracy, reliability, and availability by improving satellite geometry, especially in difficult terrain conditions where there are limits in sky view. The increase in the number of the observed satellites is helpful for shortening the initialization time and eliminating the existing position errors caused by the periodic regression of satellite constellations (Flohrer 2008). However, a minimum requirement for fusion of multi-GNSS data is the calibration of inter-system biases (ISB).

Currently most geodetic receivers available on the market are not calibrated, which leaves the instrument hardware delay unknown (Chen et al. 2015). It is assumed that the receiver clock will assimilate this delay in GPS-only processing. But in multi-GNSS processing the hardware delay is a system-dependent parameter (Wanninger 2012; Nadarajah et al. 2013; Odijk et al. 2013). Hence, ISB should be estimated together with the receiver clock parameter and other unknown parameters. An initial study of the GPS/BDS ISB was conducted by Nadarajah et al. (2013) for integer ambiguity resolution. Torre et al. (2014) presents an analysis of inter-system biases for GPS/BDS/GLONASS/Galileo/QZSS with different types of receivers. Moreover, ISB was applied to GPS/BDS single-frequency short baseline RTK (Zhao et al. 2014; Odolinski et al. 2015a) and long baseline relative positioning (Odolinski et al. 2015b; Wang et al. 2015). Nadarajah et al. (2014) carried out research on instantaneous attitude determination with GPS/BDS data. In the case of GPS/BDS PPP and ZTD/PWV retrieval (Li et al. 2015; Li et al. 2015a, 2015b; Lu et al. 2015), it was also necessary to take ISB into account.

The research mentioned above only refer to ISB estimation and its applications, but do not involve ISB modelling. If the ISB of GPS/BDS can be properly represented as a model, the accuracy of GPS/BDS combined positioning will be improved and the estimation time can be shortened because the ISB is considered an a priori constraint. In this contribution, we investigate the characteristics of the ISB between GPS and BDS so as to develop a short term (one week) station-dependent model. One week period (GPS week 1810) observations of 18 distributed stations from the IGS's MGEX are processed in PPP mode to estimate ISB. We apply a sliding window

median filter to remove the outliers of the original estimated ISB series (ISB_o) in order to obtain a smoothed ISB series (ISB_s). Based on the one week ISB_s (assumed true value), the station-dependent model can be expressed in the form of some periodic functions with different periods plus a quadratic function. After that, we apply frequency spectrum analysis to detect the periods of the periodic function (Mann et al. 1989). We introduce a least-squares (LS) approach to estimate the coefficients of the terms of the quadratic function and periodic functions. In order to assess the fitting accuracy of the proposed model, the ISB derived from the model (ISB_m) is compared with ISB_s. We evaluate the precision of the ISB prediction with this model on a day by day basis over the subsequent week (GPS week 1811). In order to verify the contribution of the ISB model as an a priori constraint, the convergence time and the accuracy of PPP result are tested.

We begin with a brief description of the GPS/BDS tracking data from MGEX. We then describe the PPP model for ISB estimation, the processing strategies be used in the experiments, and the method of frequency spectrum analysis and least squares (LS). The accuracy analysis of the short term ISB model and a study of the prediction quality are then presented. In this part, the convergence time and accuracy of PPP result with a priori constraint of ISB are also discussed. Finally, the summary and conclusions is given .

GPS/BDS Tracking data

At the time GPS launched its modernization program, China independently established the BeiDou Navigation Satellite System (BDS). The two-phase schedule enables its rapid evolution to a global system starting with providing regional coverage around the Asia-Pacific area. The initial satellite system was operational by the end of 2012. It consists of five geostationary orbit satellites (GEO), four medium earth orbit satellites (MEO) and six inclined geosynchronous orbit satellites (IGSO). BeiDou-3 M1, which is the first one of next-generation BeiDou satellites, was launched into an IGSO orbit on March 30, 2015 (http://en.beidou.gov.cn/). An operational global navigation satellite system will be available from around 2020 (Yang et al. 2011).

The MGEX is an IGS project to track, collate, and analyze all available GNSS signals. This includes data from GPS, GLONASS, BeiDou, and Galileo, Quasi-Zenith Satellite System (QZSS), the Indian Regional Navigation Satellite System (IRNSS) and space-based augmentation systems (SBAS). Over several years development, a network of multi-GNSS monitoring stations has been deployed around the globe in parallel to the legacy IGS network for GPS and GLONASS. The MGEX network has now grown to more than 100 stations and it provides an excellent opportunity to track multi-GNSS constellations and to conduct tracking data analysis. At the time of preparation for this study, about 30 stations are capable of making GPS and BDS observations (Montenbruck et al. 2013).

GPS and BDS observations during GPS week 1810 (7 days from Sept. 14 - 20,

2014) of 18 stations from the MGEX network are processed in PPP mode for ISB estimation and modelling. The observations during GPS week 1811 (7 days from Sept. 21 27, 2014) are used for assessing the accuracy of the prediction model. The distribution of the GPS and BDS tracking stations is shown in Figure 1.

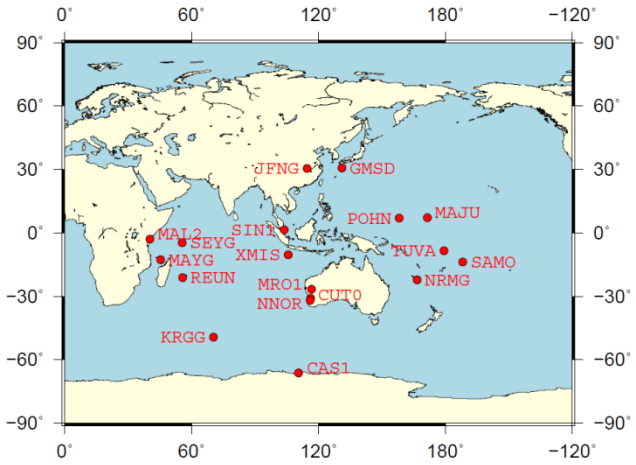

Fig. 1 Distribution of GPS/BDS stations in the MGEX network

Estimation model and processing strategy

Here the PPP solution model is applied for ISB estimation, which can be derived together with other unknown parameters. We use an extended Kalman filter to estimate the ISB as a piece-wise constant every 30 min. Afterwards the ISB can be modelled as a quadratic function plus several periodic functions. Hence we employ a frequency spectrum method to detect the different periods of periodic functions. LS is applied to determine the coefficients of both types of functions.

GPS/BDS PPP model for ISB estimation

In general, the ionospheric-free (IF) pseudorange and phase observations are utilized in PPP to eliminate the first-order effect of the ionosphere. The observation equations can be written as (Kouba 2009):

$$\begin{aligned} P &= \rho + c\cdot(dt_r - dt^s) + (b_r - b^s) + T + \tau_P \\ L &= \rho + c\cdot(dt_r - dt^s) + (B_r - B^s) + T + N + \tau_L \end{aligned} \tag{1}$$

where P and L are the ionospheric-free combination of pseudorange and carrier phase, respectively, c is the speed of light, dt_r and dt^s denote the receiver and satellite clock biases, b_r, b^s and B_r, B^s are the pseudorange and carrier phase hardware delay biases of the ionospheric-free function for receivers and satellites, T is the tropospheric delay, N is the phase ambiguity in units of meters; τ_P and τ_L

denote unmodelled parameters (e.g. the measurement noise and multipath errors for pseudorange and carrier phase), and ρ denotes the geometric distance between the phase centers of the satellite and the receiver antennas at the signal transmission and reception time, respectively. The phase center offset and variation, relativistic effects, tidal loading, ocean tide, earth rotation effects, and phase wind-up must be corrected for according to existing models (Kouba 2009), although they are not explicitly included in the equations.

For GNSS observations, the pseudorange hardware delay biases b_r, b^s are assimilated into the clock offset $c\cdot(dt_r - dt^s)$. In most GNSS data processing, the carrier phase hardware delay biases B_r, B^s are not considered. The carrier phase hardware delay bias is satellite-dependent and stable over time, thus it is absorbed by the ambiguity (Defraigne et al. 2007; Geng et al. 2012). Upon using precise satellite orbits and clocks, equation (1) can be rewritten as:

$$\begin{aligned} P &= \rho + c\cdot\overline{dt_r} + T + \tau_P \\ L &= \rho + c\cdot\overline{dt_r} + T + \overline{N} + \tau_L \end{aligned} \tag{2}$$

where $\overline{dt_r}$ and $\overline{N}$ are the modified receiver clock and ambiguity:

$$\begin{aligned} c\cdot\overline{dt_r} &= c\cdot dt_r + b_r \\ \overline{N} &= N + B_r - b_r \end{aligned} \tag{3}$$

Equation (2) indicates the PPP observation equation, in which the satellite hardware delays can be removed when applying the precise satellite clocks (Defraigne et al. 2007). From (3) we see that the ambiguity is not an integer as it contains the bias term; the term $B_r - b_r$ refers to the uncalibrated phase delay (Ge et al. 2008)

GPS/BDS PPP refers to combined PPP using observations from the GPS and BDS satellite constellations, where precise satellite orbits and clock products are available accord from the MGEX analysis centers. The GPS/BDS PPP model requires the estimation of an additional inter-system bias (ISB) parameter, hence the combined observation model can be expressed as:

$$\begin{aligned} P^G &= \rho^G + c\cdot\overline{dt_r} + T + \tau_P \\ L^G &= \rho^G + c\cdot\overline{dt_r} + T + \overline{N^G} + \tau_L \\ P^C &= \rho^C + c\cdot(\overline{dt_r} + ISB) + T + \tau_P \\ L^C &= \rho^C + c\cdot(\overline{dt_r} + ISB) + T + \overline{N^C} + \tau_L \end{aligned} \tag{4}$$

where $\overline{dt_r}$ is a common item, being the receiver clock term relating to the GPS system. The superscript G and C refer to GPS and Beidou navigation system separately. The ISB is the inter-system bias parameter between GPS and BDS in

units of time. It will be modelled as an unknown parameter and estimated together with the other parameters such as coordinates and receiver clock. So we can consider the estimated parameter vector $\overline{X}$ to be:

$$\overline{X} = \left[x, y, z, \overline{dt_r}, ISB, T, \overline{N^G}, \overline{N^C} \right] \tag{5}$$

where $\overline{N^G}$, $\overline{N^C}$ are modified ambiguity parameters of GPS and Beidou. An extended Kalman filter is employed to estimate the unknown parameters in the processing.

The estimation of the ISB parameter can be performed in three different ways: as epoch-wise variable, piece-wise constant, or daily constant. For rigorous data analysis, ISB should be estimated on an epoch-wise basis. However this approach will introduce too many unknown parameters and reduce the efficiency of the solution. Paziewski et al. (2015) made a detailed analysis of ISB estimation using double-difference measurements from various receivers. They reported that the ISB values estimated as a constant parameter for "longer pieces" showed better repeatability than when estimating an epoch-varying parameter. Considering not only the current PPP accuracy limits, but also the computing speed, we choose the piece-wise constant ISB model as the optimal approach.

During preprocessing we detect and repair clock jumps in order to avoid the misidentifying an observation jump caused by the receiver clock jump as a cycle slip. Then the Geometry-Free (GF) and Hatch-Melbourne-Wubbena (HMW) (Hatch 1982) combinations are used to detect cycle slips. An extended Kalman filter (EKF) is employed to estimate the unknown parameters. A cutoff elevation angle of 7° and an elevation-dependent weighting method are applied. MGEX precise satellite orbits and clocks from the GFZ analysis center are used in the GPS/BDS PPP processing. The tropospheric delay is corrected for its dry component using the Saastamoinen model, while the residual zenith wet delay is estimated as a random-walk process. We apply the Global Mapping Function (GMF) (Boehm et al. 2006) to convert zenith delay to slant delay. Moreover, the phase-wind up effects (Wu et al. 1992), the solid earth tide, the ocean loading tide (Petit et al. 2010) and relativistic effects are also considered. However, the satellite phase center variation (PCV) and the receiver phase center offset (PCO) and PCV corrections for BDS are not applied since they are not yet known to sufficient accuracy. Table 1 summarizes GPS/BDS observation models and data processing strategies.

Table 1 Observation models and data processing strategies for GPS/BDS PPP

Item	Models and Strategies
Tracking data	18 stations of MGEX network with GPS/BDS observations
Estimator	Extended Kalman filter (EKF)
Observations	Undifferenced ionospheric-free code and phase combination

Signal selection	GPS: L1/L2, BDS: B1/B2
Elevation angle cutoff	7°
Sampling rate	30s
Precise obit	Fixed, MGEX precise ephemeris from GFZ 15min
Precise clock biases	Fixed, MGEX combined precise clock from GFZ 5min
Observation weight	Elevation dependent weight
Tropospheric delay	Saastamoinen model & random walk process
Mapping function	Global Mapping Function (GMF)
Ionospheric delay	First order effect eliminated by ionospheric-free linear combination
Phase-windup effect	Corrected
Earth rotation	Fixed, IGS ERP product
Satellite Antenna PCO & PCV	Applied for GPS; PCO applied for BDS
Receiver Antenna PCO & PCV	Applied for GPS; not applied for BDS
Relativistic effects	IERS Convention 2010
Solid Earth tides	IERS Convention 2010
Pole tides	IERS Convention 2010
Ocean tides	IERS Convention 2010
Receiver clock biases	Estimated as white noise for each epoch
Phase ambiguity	Estimated as constant for each ambiguity arc
Time system	GPS Time
Terrestrial frame	ITRF2008
ISB	Estimated as a piece-wise constant every 30min

ISB modelling and coefficients estimation

Taking the characteristic of ISB into account, the fitting model can be expressed as a sum of a quadratic function and several periodic functions. We apply frequency spectrum analysis to detect the different periods of the periodic functions. The frequency spectrum can be generated via a Fourier transform of the time-domain signal, and the resulting values are usually presented as amplitude versus frequency (Mann et al. 1989). Any signal that can be represented by an amplitude that varies with time has a corresponding frequency spectrum. In this study, we use a fast Fourier transform (FFT) to analyze the ISB signal frequency spectrum. FFT, an algorithm to compute the discrete Fourier transform (DFT) and its inverse, rapidly converts time to

frequency and vice versa (Bergland 1969). The specific algorithm of FFT refers to (Duhamel et al. 1990).

After the periods have been detected, LS is applied to determine the coefficients of the periodic functions together and the quadratic function. Due to the application of the sliding window median filter, we can obtain a clean ISB set of values without outliers. Hence, LS is suitable to estimate the unknown coefficients. However, it is recommended to apply robust least-squares (Zhou 1989; Yang et al. 2002), on account of its outstanding capacity for data quality control (outliers detecting and repairing).

Analysis and Results

In this part, the accuracy of the PPP model for ISB estimation is analyzed. We also obtain a short term model of ISB and the derived ISB, which is compared with the true value. The comparison shows that the derived ISB from the model agrees well with the true value. Then the predicted accuracy of the model is tested. In the end, the convergence time and positioning accuracy are both studied.

Accuracy of PPP

As a first step the accuracy of the PPP solution which will affect the accuracy of the ISB should be evaluated. Hence high-precise PPP is a precondition for ISB estimation. In order to assess the accuracy of the GPS/BDS PPP processing, we processed the aforementioned 18 stations from the MGEX network for the period of GPS week 1810. All the data are processed at the 30-sec sampling interval. We compared the daily position estimates with the IGS daily solutions in north, east, and up components. RMS statistics of the residuals between GPS/BDS daily static PPP and the IGS daily solution are used to assess the external positioning precision.

As example, Figure 2 shows the mean RMS values of the differences between the GPS/BDS daily static PPP and the IGS daily solution for week 1810 at seven stations (CAS1, MAJU, MAL2, NNOR, REUN, TUVA, and XMIS). In this plot, the averaged RMS of the north and east components are 0.26-0.80 cm and 0.70-1.78 cm respectively, which confirms that the PPP solution has a horizontal accuracy of better than 2 cm. The mean RMS of the up component is 1.43-5.86 cm, but even more than half of all stations are better than 2 cm.

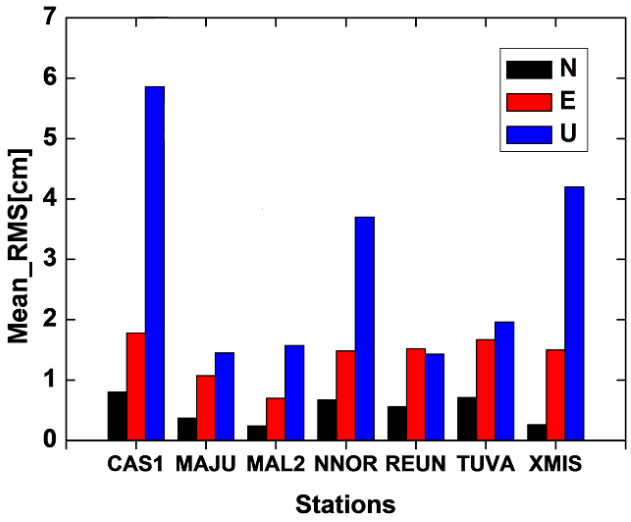

Fig. 2 Mean RMS statistics of coordinate differences between GPS/BDS daily static PPP and IGS daily solution for each station in north, east and up components over GPS week 1810.

The daily statistic of the whole week are summarized in Table 2, which shows not only the errors between the daily PPP results and the IGS daily solution in week 1810 for seven stations, but also the mean error of each station and the whole week period. The daily comparison for MAJU station on the fifth day of week 1810 is blank, because there is no positioning result for the station in the SINEX file provided by IGS on that day. We can see that the mean RMS values of all stations during one week are 0.51 cm, 1.38cm, and 2.88 cm for the north, east and up components, respectively. The mean RMS of all stations further confirms the high accuracy of the GPS/BDS PPP processing.

Table 2 Daily and mean RMS of residuals of the PPP position estimates against the IGS daily solutions for GPS week 1810 (unit: cm)

Day of week 1810		1	2	3	4	5	6	7	Mean
CAS1	N	0.84	0.56	1.31	0.49	1.33	0.47	0.66	0.80
	E	1.85	2.33	2.58	0.59	1.95	2.04	1.16	1.78
	U	4.95	6.83	6.28	6.88	5.08	6.42	4.61	5.86
MAJU	N	0.30	0.38	0.83	0.22		0.39	0.14	0.37
	E	0.87	1.49	0.48	0.86		1.30	1.46	1.07
	U	2.34	0.55	0.99	1.68		0.24	2.91	1.45
MAL2	N	0.22	0.09	0.21	0.39	0.05	0.7	0.07	0.24
	E	1.02	0.37	0.37	1.81	0.83	0.16	0.38	0.70
	U	2.08	1.88	2.43	0.72	2.56	0.53	0.83	1.57

	N	0.6	0.86	0.79	0.71	0.61	0.75	0.42	0.67
NNOR	E	2.08	1.95	1.87	0.98	0.9	1.66	0.92	1.48
	U	3.82	3.48	4.01	3.56	4.97	3.31	2.77	3.70
	N	0.73	0.79	0.74	0.56	0.4	0.4	0.32	0.56
REUN	E	1.58	1.78	1.33	1.5	1.52	1.45	1.5	1.52
	U	0.47	0.41	1.19	2.73	1.13	1.81	2.25	1.43
	N	0.75	0.65	0.67	1.05	0.26	0.75	0.85	0.71
TUVA	E	2.53	1.01	2.13	1.07	1.53	1.53	1.90	1.67
	U	3.98	3.34	2.30	1.14	0.87	0.96	1.18	1.96
	N	0.16	0.16	0.12	0.53	0.42	0.19	0.29	0.26
XMIS	E	1.18	1.28	1.07	1.23	1.4	2.19	2.18	1.50
	U	3.73	4.66	5.14	4.25	4.15	3.96	3.57	4.20
ALL	N	0.51		E	1.38		U	2.88	

ISB estimation and the short-term model

In order to evaluate the performance of ISB estimation and validate the short-term station-dependent model for ISB, we carry out the processing of 18 stations from the MGEX network for GPS week 1810 according to the processing strategy described above and summarized in Table 1. We process ISB as a piece-wise parameter every 30 mins in PPP mode.

Figure 3 shows the original ISB series (ISB_o) and the smoothed ones (ISB_s) at eight stations from the MGEX networks during GPS week 1810 as examples. The stations are CAS1, MAJU, MAL2, MAYG, NNOR, REUN, TUVA and XMIS. These stations were selected because they can observe more than four BDS satellites and have reliable and continuous data during the period under consideration. The receiver types and firmware versions of the eight stations are shown in Table 3, where one can see that the receiver models of Trimble NetR9 and SEPT POLARX4 are widely installed at MGEX stations. The ISB_o and ISB_s are displayed in blue and red colors respectively. It should be noted that the ISB_o has many outliers and considerable noise. Therefore we apply a sliding window median filter to generate the smoothed ISB series, because the median has good capability of rejecting outliers. It is obvious that the filtered ISB series is more robust and smoother than the original series. The sliding window median filter can effectively remove the outliers and improve the reliability of the estimated ISB. From the characteristics of ISB_s, the model for ISB

can be approximated by a quadratic function plus some periodic functions.

Table 3 Stations and receiver types at 8 stations under consideration

Station ID	Receiver type/ Firmware version
CAS1	Trimble NetR9 4.81
MAJU	Trimble NetR9 4.81
MAL2	SEPT POLARX4 2.5.1p1
MAYG	TRIMBLE NETR9 4.85
NNOR	SEPT POLARX4 2.5.1p1
REUN	Trimble NetR9 4.85
TUVA	Trimble NetR9 4.81
XMIS	Trimble NetR9 4.85

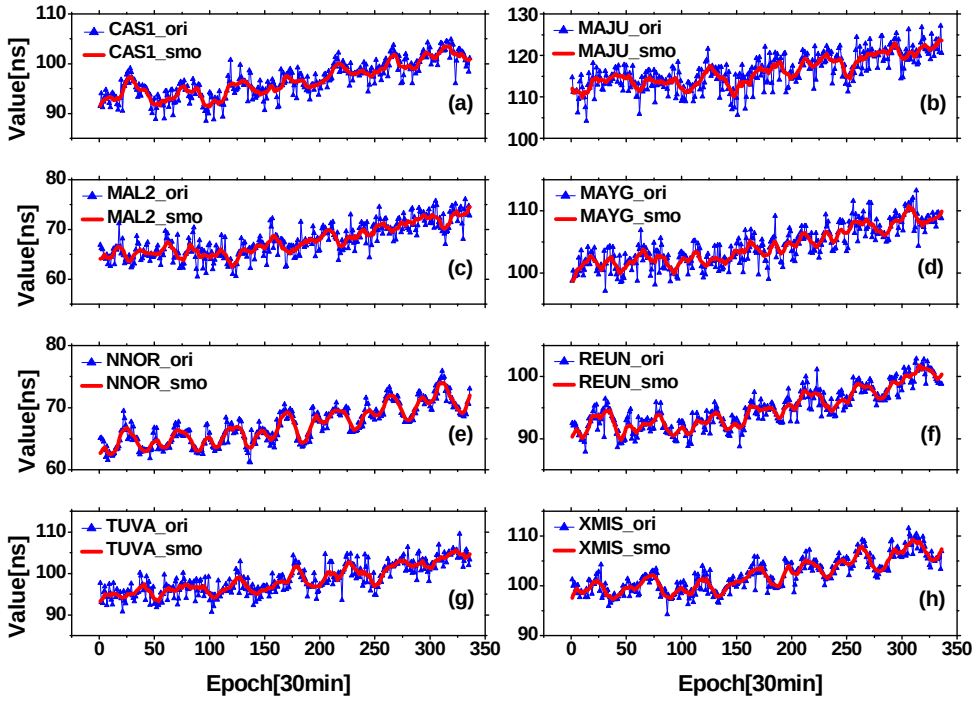

Fig. 3 Original (ori) and smoothed (smo) ISB series in nanoseconds during GPS week 1810 at stations CAS1 (a), MAJU (b), MAL2 (c), MAYG (d), NNOR (e), REUN (f), TUVA (g), and XMIS (h) for the 30 min sampling interval

In order to validate this modelling strategy, we use the approaches outlined above. The model can be represented in the following form:

$$ISB = A \cdot t^2 + B \cdot t + C + \sum_{i=1}^{n} (D_i \cdot \cos(\frac{2\pi t}{P_i}) + E_i \cdot \sin(\frac{2\pi t}{P_i})) \qquad (7)$$
$$t = T - T_{oc}$$

where A, B, and C are the coefficients of the quadratic, first-order, and constant term for the quadratic function, respectively. The symbols D_i and E_i denote the coefficients of the periodic functions, P_i are the periods of the periodic functions,

and T and T_{oc} represent the current epoch time and the reference epoch time. In this study T_{oc} is the first epoch time in GPS week 1810. The coefficients of both functions are estimated by LS and the different periods of the periodic functions are derived from frequency spectrum analysis. The results are shown in Table 4. It can be noted that GPS/BDS ISB of all eight stations has a quadratic function and two or three periodic functions, which commonly contain one day and semi-diurnal periods.

Table 4 Coefficients and periods of quadratic and periodic function at 8 stations under consideration. The value of P_i is the number of epoch with 30min interval.

Coefficient/ period	A	B	C	D_i	E_i	P_i
CAS1	0.000084	-0.000002	93.462	-1.103	-0.691	48
				0.095	0.152	24
				-0.344	-0.224	16
MAJU	0.000077	0.002091	112.964	-0.121	-1.374	48
				0.583	-0.215	24
				0.029	-0.193	33.6
MAL2	0.000096	-0.005940	65.116	0.188	0.571	48
				-0.428	-0.476	24
MAYG	0.000064	0.005136	101.026	-0.606	0.613	48
				-0.134	-0.227	24
NNOR	0.000052	0.008957	63.672	-1.332	0.374	48
				0.920	0.741	24
				0.196	0.309	16
REUN	0.000100	-0.004576	91.828	-1.136	-0.275	48
				0.019	0.223	24
				0.098	0.490	16
TUVA	0.000071	0.004595	95.025	-0.616	-1.034	48
				-0.300	-0.120	24
				-0.509	0.304	28
XMIS	0.000070	0.004422	98.845	-1.312	0.906	48
				0.775	0.490	24

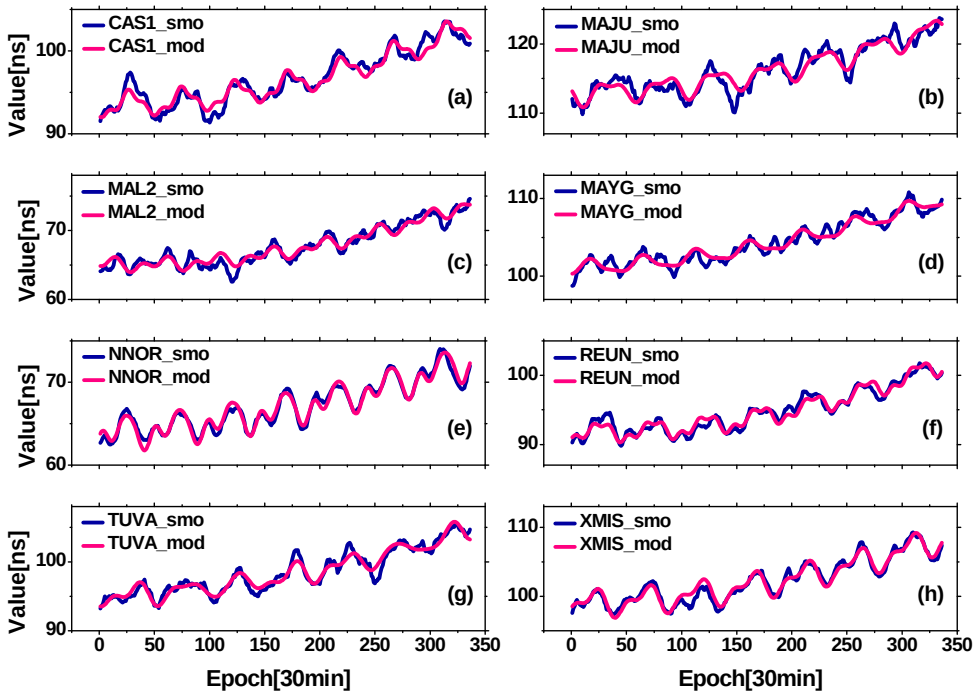

Fig. 4 Smoothed (smo) and modelled (mod) ISB series during GPS week 1810 at stations CAS1 (a), MAJU (b), MAL2 (c), MAYG (d), NNOR (e), REUN (f), TUVA (g) and XMIS (h) for the 30 min sampling interval

In order to assess the fitting accuracy of the model, we compare the ISB values derived from the model (ISB_m) with the smoothed values (assumed to be the true values). Figure 4 shows the values of ISB_s and ISB_m during the same period for the eight stations mentioned above. One can see that the modelled ISB series agree well with the smoothed series. Figure 5 shows the distribution of differences between modelled and smoothed ISB series, together with the standard normal distribution curves. It can be seen that the frequency count of the differences follows closely a normal distribution. In Table 5, the statistical results of the differences between the modelled and the smoothed ISB series are listed, where the mean values of the differences for the eight stations are 0.046 ns, 0.009 ns, -0.067 ns, 0.009 ns, -0.010 ns, 0.011 ns, -0.006 ns, and -0.069 ns, and the RMS of the differences are 0.807 ns, 1.154 ns, 0.769 ns, 0.688 ns, 0.510 ns, 0.659 ns, 0.709 ns, and 0.609ns, with an accuracy level of about 0.7 ns. This means that the model for the ISB proposed in this study has a high fitting precision and a good consistency. However, the RMS of station MAJU is obviously weaker than for the others, and the possible reason may be the higher observation noise or worse BDS geometry. These results confirm the conclusion made earlier that the model proposed in this study is precise enough, reaching a level of 0.7 ns, and can be applied to ISB prediction.

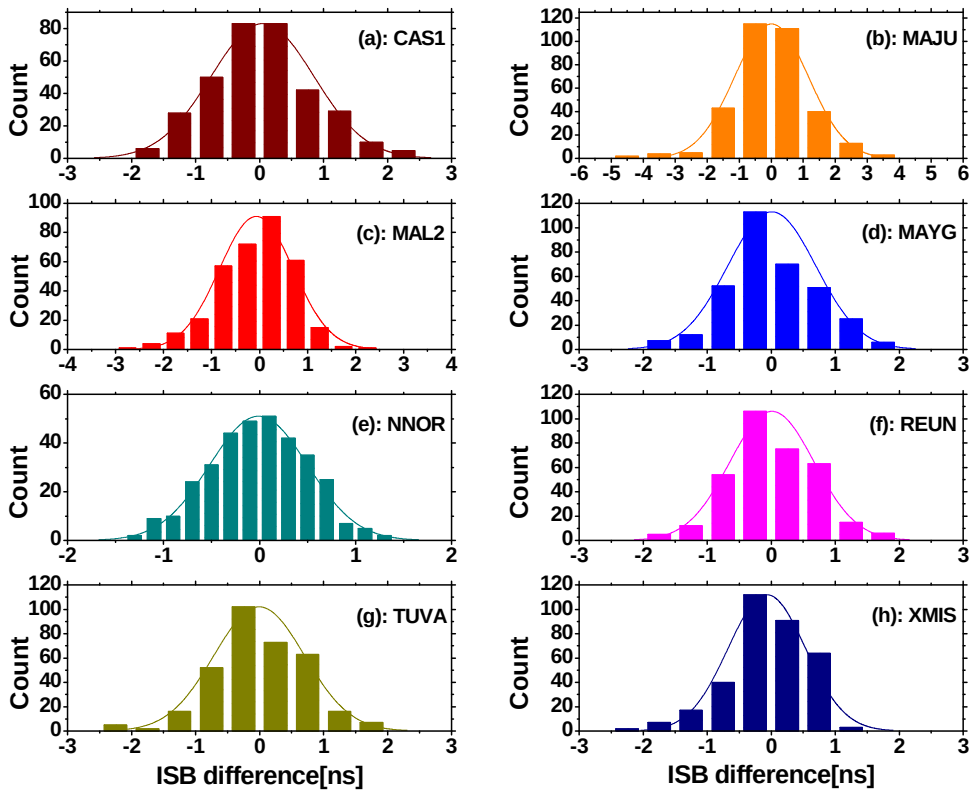

Fig. 5 Distribution of differences between modelled and smoothed ISB series during GPS week 1810 at stations CAS1 (a), MAJU (b), MAL2 (c), MAYG (d), NNOR (e), REUN (f), TUVA (g), and XMIS (h), with the standard normal distribution curves

Table 5 Statistics for differences between modelled and smoothed ISB series (units: ns)

Station ID	Max	Min	Mean	RMS
CAS1	2.237	-1.936	0.046	0.807
MAJU	3.659	-4.224	0.009	1.154
MAL2	2.179	-2.595	-0.067	0.769
MAYG	1.825	-1.676	0.009	0.688
NNOR	1.313	-1.346	-0.010	0.510
REUN	1.848	-1.897	0.011	0.659
TUVA	0.701	-2.339	-0.006	0.709
XMIS	1.447	-2.040	-0.069	0.609

ISB prediction with the model

We perform as experiment with the aforementioned eight stations during the following GPS week 1811. The predicted ISB series (ISB_p) are generated according to (7) with the variation of epoch time T. We estimate the ISB_o following the approach described above and obtain the ISB_s using the sliding window median filter. The

precision of prediction is evaluated by comparing the ISB_p with ISB_s in the corresponding period. The comparisons during the seven day period are shown in Figure 6. We can see that as time goes on, the accuracy of prediction has a tendency to degrade. During the first day, the ISB_p agrees well with ISB_s. But after this period, the agreement declines markedly, especially during the later days.

Figure 7 shows the RMS values of the ISB differences between the smoothed and predicted values for different periods from one day to seven days. One can see that the RMS of the ISB differences at the eight stations is 0.57-1.21 ns for a one day period. For the two day period they are 0.77- 1.72 ns. As the time period increases, the RMS is getting worse, which is consistent with Figure 6. The corresponding statistics are listed in Table 6. From these analyses we recommend a prediction duration of one day. The comparison of the ISB prediction further confirms the aforementioned conclusion concerning the accuracy of the proposed ISB model and its advantage for prediction purposes. It confirms the potential effects of this model for subsequent GPS/BDS PPP and POD, since the ISB derived from this model can be considered as a given value, without requiring it to be estimated or considered an a priori constraint in PPP/POD solutions. This will improve the accuracy and reduce the processing time. Furthermore, under some extreme circumstances, the standard multi-GNSS PPP model with ISB estimation may fail because of rank deficiency. For instance, in the situation when only four satellites can be observed (at least one BDS satellite), the PPP model with a known ISB may still obtain results.

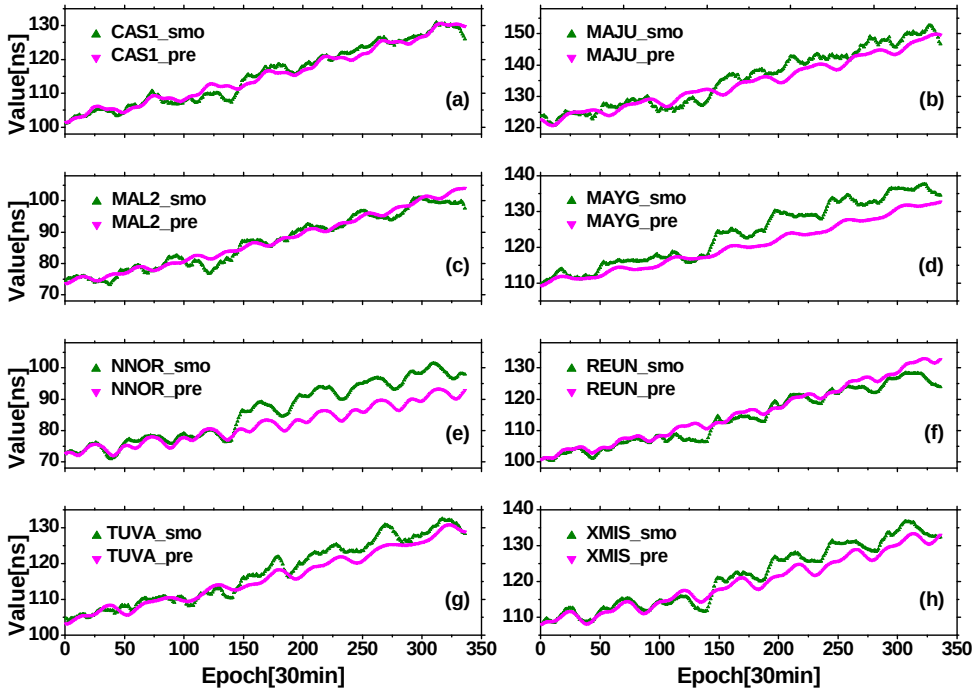

Fig. 6 ISB derived from smoothed (smo) and predicted (pre) ISB at stations CAS1 (a), MAJU (b), MAL2 (c), MAYG (d), NNOR (e), REUN (f), TUVA (g), and XMIS (h) for GPS week 1811

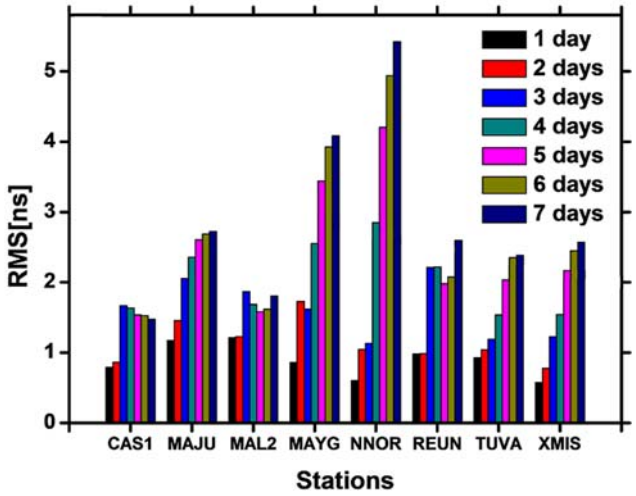

Fig. 7 RMS of ISB differences of smoothed and predicted at stations CAS1, MAJU, MAL2, MAYG, NNOR, REUN, TUVA, and XMIS for periods from one to seven days

Table 6 Statistics of the ISB differences of smoothed and predicted at stations CAS1, MAJU, MAL2, MAYG, NNOR, REUN, TUVA, and XMIS for periods from one to seven days (units: ns)

Day period	1 Day	2 Days	3 Days	4 Days	5 Days	6 Days	7 Days
CAS1	0.79	0.86	1.66	1.64	1.54	1.53	1.48
MAJU	1.17	1.45	2.05	2.35	2.60	2.68	2.72
MAL2	1.21	1.22	1.86	1.69	1.58	1.62	1.81
MAYG	0.86	1.72	1.62	2.55	3.44	3.92	4.08
NNOR	0.60	1.04	1.13	2.84	4.20	4.94	5.42
REUN	0.97	0.98	2.21	2.21	1.98	2.08	2.59
TUVA	0.92	1.04	1.19	1.53	2.03	2.34	2.38
XMIS	0.57	0.77	1.22	1.54	2.16	2.45	2.56

Analysis of convergence time and positioning accuracy

Since the average RMS of the ISB prediction on the first day of GPS week 1811 (Doy 264) is about 0.8 ns, it is not precise enough to consider the ISB as a constant parameter in the observation equation. So here it is better to treat the predicted ISB as an a priori constraint. The a priori value of ISB is used with the predicted ISB of each station mentioned above, and the a priori precision is applied with the RMS of ISB

model. In order to verify the improvement of this a priori constraint, the convergence time and accuracy of PPP with and without a priori constraint are compared. The error, which is derived from the difference between PPP result and truth value, is analyzed for convergence time and accuracy of PPP.

With respect to the analysis of convergence time, primarily we define the convergence criterion as the moment when the error of positioning is less than 0.1m in each component of north (N), east (E), and up (U). After the convergence epoch has been found, considering the reliability of the criterion, it is necessary to check the errors of following 20 epochs. If they are all below 0.1 m, the current epoch can be identified as the true convergence time. Figure 8 shows the comparison of convergence time without and with a priori constraint of ISB. It can be seen that the average convergence time of the PPP processing without ISB constraint are 28.5, 43.4, and 50.8 min in N, E, and U components, respectively. When using the predicted ISB as an a priori constraint, the mean convergence time in three components are 22.9, 36.4, and 49.6 min, respectively. Therefore, the convergence speed can be increased by 19.6%, 16.1%, and 2.4%, respectively.

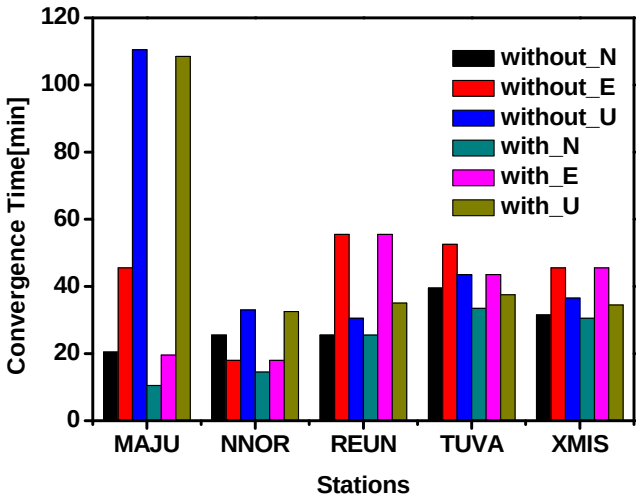

Fig. 8 Comparison of the Convergence time between without and with a priori constraint in N, E, and U components at stations MAJU, NNOR, REUN, TUVA, and XMIS on Doy 264. Convergence time is defined as the time when the position error in a given component is less than 0.1 m.

As for the accuracy of PPP, we also compare the results of the cases with and without a priori constraint. The statistics of RMS are shown in Table 7. From which we can see that the mean RMS of PPP processing without a priori constraint are 0.48, 2.02, and 2.86 cm in N, E, and U components, respectively. After adding the a priori constraint, the average RMS become 0.46, 1.78, and 2.92 cm in three components, respectively. Thus it can be concluded that when using predicted ISB as an a priori constraint, the accuracy of positioning in N and U components are similar as obtained without a priori constraint, but the E component improves by 11.9%. It is obvious that with the a priori constraint of ISB can mainly improve the positioning accuracy in E component.

Table 7 The positioning RMS of with and without a priori constraint at stations MAJU, NNOR, REUN, TUVA, and XMIS on Doy 264 (units: cm)

Station	Without			With		
	N	E	U	N	E	U
MAJU	0.4	1.0	3.1	0.4	1.1	3.2
NNOR	0.5	1.2	2.5	0.5	0.8	2.4
REUN	0.7	1.5	3.4	0.6	1.3	3.6
TUVA	0.5	2.7	1.9	0.6	2.8	1.9
XMIS	0.3	3.7	3.4	0.2	2.9	3.5
Average	0.48	2.02	2.86	0.46	1.78	2.92

Summary and Conclusions

ISB is known to affect the combined precise positioning and precise orbit determination of multi-GNSS observations. Normally, ISB is considered an unknown parameter and estimated together with other parameters in PPP/POD solutions. In this contribution, we have developed a short-term ISB model relating GPS and BDS. The GPS and BDS data during GPS week 1810 from 18 stations of the MGEX network are processed in a PPP model in order to estimate the original ISB series (ISB_o). We apply a sliding window median filter to remove outliers from ISB_o and generate smoothed ISB series (ISB_s). After analyzing the characteristics of the ISB we propose a short-term ISB model for a one week period, which contains a quadratic function with quadratic-term, first-order-term and constant-term, and two or three periodic functions with one day and semi-diurnal periods.

In order to determine the periods of the periodic function and the coefficients of the quadratic function and the periodic functions, we apply a frequency spectrum analysis and use the least squares approach, respectively. Then we compare the ISB_m with ISB_s to verify the model. It was noted that the differences closely follow a normal distribution. The results also show that ISB derived from model (ISB_m) agree well with ISB_s. The RMS values of the differences between ISB_m and ISB_s are at an accuracy level of 0.7 ns, and the mean values of differences for eight stations are from -0.069 to 0.046 ns. The agreement implies that the short-term ISB model proposed has a high fitting accuracy and is effective for ISB prediction.

Data from the following week (GPS week 1811) for the above mentioned stations are processed using ISB values that were predicted from the model. Comparing the predicted ISB series (ISB_p) with ISB_s, we conclude that the prediction accuracy during the one week period drops by the day. The RMS values for the one day period differences can reach 0.57-1.21 ns, but those for two days period degrade to 0.77-1.72 ns. Thus we recommend a predicting duration of one day. The results further confirm the performance of the derived short-term model and the benefit of applying it for ISB prediction. There are benefits in using this model for subsequent GPS/BDS PPP and

POD, since the ISB derived from this model can be applied as an a priori constraint in these solutions. This effectively improves the result accuracy in E component by 11.9%. In addition, the processing time is shortened by 19.6%, 16.1%, and 2.4% in N, E, and U components, respectively. Furthermore, under some extreme circumstances without sufficient observations, the GPS/BDS PPP model with an a priori constraint of ISB may still obtain results because it avoids the rank deficiency that otherwise would arise if ISB has to be estimated.

Acknowledgments This study is supported by the Chinese Scholarship Council, Technical University of Berlin, German Research Centre for Geosciences Potsdam, and Institute of Space Sciences of Shandong University. This work is supported by the National Natural Science Foundation of China (41574013, 41574025, and 41174008). The authors would like to thank IGS and MGEX for providing the GPS and BDS data. Thanks also go to three reviewers for their valuable comments which have improved this paper considerably.

References

Bergland G D (1969) A guided tour of the fast Fourier transform. IEEE Spectrum 6(7): 41-52. doi: 10.1109/mspec.1969.5213896

Boehm J, Niell A, Tregoning P, Schuh H (2006) Global Mapping Function (GMF): A new empirical mapping function based on numerical weather model data. Geophysical Research Letters 33(7). doi: 10.1029/2005gl025546

Chen J P, Zhang Y Z, Wang J G, Yang S N, Dong D A, Wang J X, Qu W J, Wu B (2015) A simplified and unified model of multi-GNSS precise point positioning. Adv Space Res 55(1): 125-134. doi: DOI 10.1016/j.asr.2014.10.002

Defraigne P, Bruyninx C, Guyennon N. (2007). GLONASS and GPS PPP for time and frequency transfer. In: Proceedings of the EFTF '07, Geneva, Switzerland.

Duhamel P, Vetterli M (1990) Fast Fourier-Transforms - a Tutorial Review and a State-of-the-Art. Signal Processing 19(4): 259-299. doi: Doi 10.1016/0165-1684(90)90158-U

Flohrer C (2008) Mutual Validation of Satellite-geodetic Techniques and Its Impact on GNSS Orbit Modeling. Geodätisch-geophysikalische Arbeiten in der Schweiz, Vol 75.

Ge M, Gendt G, Rothacher M, Shi C, Liu J (2008) Resolution of GPS carrier-phase ambiguities in Precise Point Positioning (PPP) with daily observations. Journal of Geodesy 82(7): 389-399. doi: DOI 10.1007/s00190-007-0187-4

Geng J H, Shi C, Ge M R, Dodson A H, Lou Y D, Zhao Q L, Liu J N (2012) Improving the estimation of fractional-cycle biases for ambiguity resolution in precise point positioning. Journal of Geodesy 86(8): 579-589. doi: DOI 10.1007/s00190-011-0537-0

Hatch R (1982) The Synergism of GPS Code and Carrier Measurements. Proceedings of the Third International Symposium on Satellite Doppler Positioning at

Physical Sciences Laboratory of New Mexico State University, Feb. 8-12, Vol. 2, pp 1213-1231.

Kouba J (2009) A guide to using International GNSS Service (IGS) Products. International GNSS Service (IGS).

Li M, Li W W, Shi C, Zhao Q L, Su X, Qu L Z, Liu Z Z (2015) Assessment of precipitable water vapor derived from ground-based BeiDou observations with Precise Point Positioning approach. Adv Space Res 55(1): 150-162.

Li X, Ge M, Dai X, Ren X, Fritsche M, Wickert J, Schuh H (2015a) Accuracy and reliability of multi-GNSS real-time precise positioning: GPS, GLONASS, BeiDou, and Galileo. Journal of Geodesy 89(6): 607-635. doi: 10.1007/s00190-015-0802-8

Li X, Zhang X, Ren X, Fritsche M, Wickert J, Schuh H (2015b) Precise positioning with current multi-constellation Global Navigation Satellite Systems: GPS, GLONASS, Galileo and BeiDou. Sci Rep 5: 8328. doi: 10.1038/srep08328

Lu C, Li X, Nilsson T, Ning T, Heinkelmann R, Ge M, Glaser S, Schuh H (2015) Real-time retrieval of precipitable water vapor from GPS and BeiDou observations. Journal of Geodesy. doi: 10.1007/s00190-015-0818-0

Mann K A, Werner F W, Palmer A K (1989) Frequency spectrum analysis of wrist motion for activities of daily living. Journal of orthopaedic research : official publication of the Orthopaedic Research Society 7(2): 304-306. doi: 10.1002/jor.1100070219

Montenbruck O, Steigenberger P, Khachikyan R, Weber G, Langley RB, Mervart L, Hugentobler U (2013) IGS-MGEX: preparing the ground for multi-constellation GNSS science. In: 4th international colloquium on scientific and fundamental aspects of the Galileo system, 4–6 December 2013, Prague, CZ

Nadarajah N, Teunissen P J G, Raziq N (2013) BeiDou Inter-Satellite-Type Bias Evaluation and Calibration for Mixed Receiver Attitude Determination. Sensors-Basel 13(7): 9435-9463.

Nadarajah N, Teunissen P J G, Raziq N (2014) Instantaneous BeiDou-GPS attitude determination: A performance analysis. Adv Space Res 54(5): 851-862.

Odijk D, Teunissen P J G (2013) Characterization of between-receiver GPS-Galileo inter-system biases and their effect on mixed ambiguity resolution. GPS Solut 17(4): 521-533. doi: DOI 10.1007/s10291-012-0298-0

Odolinski R, Teunissen P J G, Odijk D (2015a) Combined BDS, Galileo, QZSS and GPS single-frequency RTK. Gps Solut 19(1): 151-163.

Odolinski R, Teunissen P J G, Odijk D (2015b) Combined GPS plus BDS for short to long baseline RTK positioning. Meas Sci Technol 26(4).

Paziewski J, Wielgosz P (2015) Accounting for Galileo-GPS inter-system biases in precise satellite positioning. Journal of Geodesy 89(1): 81-93. doi: DOI 10.1007/s00190-014-0763-3

Petit G, Luzum B. (2010). IERS Conventions (2010). In: Proceedings of the IERS Technical Note 36. Verlag des Bundesamts für Kartographie und Geodäsie, Frankfurt am Main.

Torre A D, Caporali A (2014) An analysis of intersystem biases for multi-GNSS

positioning. Gps Solut 19(2): 297-307. doi: 10.1007/s10291-014-0388-2
Wang M, Cai H Z, Pan Z P (2015) BDS/GPS relative positioning for long baseline with undifferenced observations. Adv Space Res 55(1): 113-124.
Wanninger L (2012) Carrier-phase inter-frequency biases of GLONASS receivers. Journal of Geodesy 86(2): 139-148. doi: DOI 10.1007/s00190-011-0502-y
Wu J, Wu S, Hajj G, Bertiger W, Lichten S (1992) Effects of antenna orientation on GPS carrier phase. Astrodynamics 1: 1647-1660.
Yang Y, Song L, Xu T (2002) Robust estimator for correlated observations based on bifactor equivalent weights. Journal of Geodesy 76(6-7): 353-358. doi: DOI 10.1007/s00190-002-0256-7
Yang Y X, Li J L, Xu J Y, Tang J, Guo H R, He H B (2011) Contribution of the Compass satellite navigation system to global PNT users. Chinese Sci Bull 56(26): 2813-2819. doi: DOI 10.1007/s11434-011-4627-4
Zhao S H, Cui X W, Guan F, Lu M Q (2014) A Kalman Filter-Based Short Baseline RTK Algorithm for Single-Frequency Combination of GPS and BDS. Sensors-Basel 14(8): 15415-15433.
Zhou J (1989) Classical Theory of Errors and Robust Estimation. Acta Geodaetica et Cartographica Sinica 18(2): 115-120.

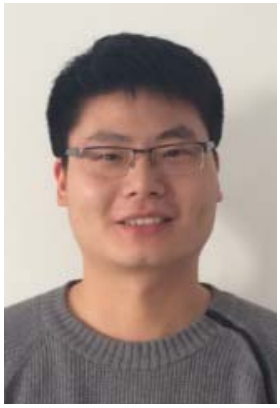

Nan Jiang has been a Ph.D. candidate in Technical University Berlin (TU Berlin) and GFZ since 2013. He received his MS degree in Chang'an University of China in 2013. His current research mainly involves the algorithms of multi-GNSS inter system bias.

Yan Xu is a Ph.D. candidate of Technical University Berlin (TU Berlin) and GFZ. She received her master's degree in Chang'an University of China in 2012. The focus of her current research is in high precision GNSS processing and its application.

Prof. Dr. Tianhe Xu received his Ph.D. and MS degrees in Geodesy from the Zhengzhou Institute of Surveying and Mapping of China in 2004 and 2001. He worked in the GFZ as a visiting scientist from 2009 to 2011. Currently, he is a professor in the Xi'an Research Institute of Surveying and Mapping and State Key Laboratory of Geo-Information Engineering in Xi'an, China. His research interests are satellite navigation, orbit determination, satellite gravity data processing and quality control.

Prof. Dr. Guochang Xu obtained his Ph.D. from the Technical University Berlin in 1992. Having worked as a scientist at the GFZ from 1993 to 1998 and as a senior scientist at the National Survey and Cadastre, Denmark, from 1998 to 1999, he returned to GFZ as a senior scientist in 1999. In 2014 he was honored as the National distinguished professor by Shangdong University and currently works in the Institute of Space Sciences in Shangdong University at Weihai. He is the author of the books GPS (2003, 2007, 2011 Chn Ed., 2014, Persian Ed.) and Orbits (2008, 2013).

Mr. Zhangzhen Sun received his MS degree in Geodesy and Surveying Engineering from the Chang'an University in 2013. Currently, he is an engineer in Institute of Space Science Shandong University at Weihai, China. His research interests are satellite navigation, orbit determination and prediction of Earth Rotation Parameters.

Prof. Harald Schuh received his Ph.D. degree at University of Bonn Germany in 1986. He is currently the Director of Dept. 1 "Geodesy and Remote Sensing" at GFZ, and the professor for "Satellite Geodesy" at Technical University Berlin (TU Berlin). In this year he was elected as the president of the International Association Geodesy (IAG). His research interests are VLBI technique and its applications.